4690 *Macromolecules* **2009**, *42*, 4690–4700
DOI: 10.1021/ma900644t

Macromolecules
ARTICLE

# Origin of the α, β, (βα), and "Slow" Dielectric Processes in Poly(ethyl methacrylate)

**K. Mpoukouvalas[†] and G. Floudas***

*University of Ioannina, Department of Physics, and Foundation for Research and Technology-Hellas (FORTH), Biomedical Research Institute (BRI), P.O. Box 1186, 451 10 Ioannina, Greece*

**G. Williams***

*University of Wales Swansea, Singleton Park, Swansea SA2 8PP, U.K.*
*[†] Present address: Max-Planck-Institut fur Polymerforschung, D-55021 Mainz, Germany*

*Received March 25, 2009; Revised Manuscript Received April 22, 2009*

ABSTRACT: The dynamics in poly(ethyl methacrylate) (PEMA) was studied as a function of temperature (in the range from 133.15 to 453.15 K), pressure (0.1 to 300 MPa), and molecular weight ($2.0 \times 10^3$ and $1.59 \times 10^4$ g/mol) for frequencies from $3 \times 10^{-3}$ to $10^6$ Hz using dielectric spectroscopy (DS). In addition, rheological studies were made within the temperature range from 323.15 to 383.15 K. The studies reveal four dielectrically active processes—α, β, αβ, and "slow". On lowering the temperature or increasing the applied pressure the αβ process is transformed into α and β processes. The relaxation strength of the β-process decreases markedly with increasing pressure (both above and below the glass temperature, $T_g$) and, for $T > T_g$, is accompanied by a complementary increase in relaxation strength of the α-process. The origins of the four dielectrically active processes are discussed in terms of the (i) apparent activation volume and (ii) values of the ratio of activation energies at constant volume and pressure. The latter allowed discussion of the relative contributions of thermal energy and volume to each of the dynamic processes. As a part of the paper, we derive the canonical set of equations that describe the effects of the thermodynamic variables $P$, $V$, $T$ on the average relaxation times and these are employed to aid the interpretations of the origins of the individual relaxation processes.

## I. Introduction

Poly(*n*-alkyl methacrylate)s are useful materials with applications in packaging, medicine, and in textile, paper and paint industries. These applications rely on their unique combination of high optical transparency (contact lenses), weather and heat resistance and good mechanical and electrical properties. In addition, they have attracted the interest of the scientific community because of their rich dynamics[1−21] and unique heterogeneous nanostructure.[11,13,14,18] There have been many publications concerning multiple relaxations in poly(alkyl methacrylates) and related polymers, including those by Ishida[2,8] Williams,[4] Beiner,[13,14,19] Floudas,[11] Ngai,[19] Spiess,[16−18,20] and their co-workers. Furthermore, it has been proposed[13,14] that higher *n*-alkyl members of the series are composed of nanosegregated main chains and side groups and that this gives rise to two glass temperatures−one associated with the backbone and the other with polyethylene-like dynamics within the alkyl nanodomains. In contrast to polymers in which dipolar groups are rigidly attached to the main-chain, e.g. as in aromatic polyesters and polycarbonates,[1] the poly(alkylmethacrylates) have, in addition, dipole-components in the ester side-group that are flexibly attached to the main chain and which can undergo motions not requiring extensive accompanying motions of the main-chains. These side-group motions give rise to a β-relaxation process[1−22] in addition to the primary α-relaxation associated with the glass-transition of a polymer. The unusual dielectric properties of poly(n-alkyl methacrylates) were first observed by Ishida and Yamafuji[2] and discussed by McCrum, Read, and Williams[1] who noted (i) the relaxation strength of the dielectric β-process can exceed that of the α-process (as in the case of a-poly(methyl methacrylate)), (ii) the β-process is observed above the apparent glass-transition temperature $T_g$, and (iii) α- and β-processes coalesce to form the βα-process at high temperatures. The behavior of PEMA (see Figure 8.19 in ref 1, p 267) prompted Williams[4] to study its dielectric properties over a range of temperature and applied pressure. The merging/coalescence of the α and β processes to form the βα-process was observed as the temperature was raised at ambient pressure and demerging ("decoalescence") was achieved by application of a hydrostatic pressure. This work established the general pattern, $\alpha,\beta \rightarrow \beta\alpha$ observed for many amorphous polymers, especially the poly(alkyl methacrylates).[6,13,16−19,22,23] The complex relaxation behavior of the latter polymers made clear the need to obtain interpretations of dielectric relaxation behavior based on the molecular properties and molecular dynamics of chains. Dielectric relaxations in these materials arise (see Appendix) from the motions of dipole components $\mu_b$ fixed rigidly to the chain backbone, which move when the backbone moves (α-process), and components $\mu_s$ contained in the flexible ester side groups which, below coalescence, can move fairly independently of, or in concert with, slight motions of, the chain backbone, giving the β-process or, above coalescence, in concert with the overall motions of the backbone, giving the βα-process. The α-process relaxes the relaxation strength that remains after the β-process has taken place. The dielectric relaxation strengths of backbone and side-chain motions can be determined from knowledge of $\mu_b$ and $\mu_c$ and

*Corresponding authors. E-mail: (G.F.) gfloudas@cc.uoi.gr; (G.W.) g.williams6013@ntlworld.com

 Published on Web 05/08/2009 

the overall spatial-extents of motion for the $\beta$-process, thus giving a molecular basis, rather than a phenomenological one, for the dielectric relaxations in these polymers.

Among the different thermodynamic variables, applied pressure is of considerable importance in studying polymer dynamics.[4−8,22−25] For example, earlier studies of application of pressure have shown[4] that this is the right variable if a separation of the segmental ($\alpha$-) from the more local $\beta$-process is needed. Pressure, is also of key importance in identifying the main control-parameter that dominates the slow dynamics in amorphous polymers and glass-forming liquids and gives rise to the dynamic arrest at the glass temperature, $T_g$. With respect to the liquid-to-glass transformation, theoretical predictions consider as extreme cases: (a) thermally activated processes on a constant-density "energy landscape"[26,27] and (b) free-volume theories.[28] Since changing $T$ affects both the thermal energy and the volume, it is impossible to separate the two effects by $T$ alone. In order to disentangle the effects of $T$ and $V$ on the dynamics, pressure-dependent measurements are of paramount importance, since $P$ can be applied isothermally (affecting only $V$). It has been proposed many years ago[3,4,29] that the ratio $\mathscr{R}$ of the apparent activation energy at constant volume, $Q_V = \mathrm{R}(\partial[\ln\tau]/\partial(1/T))_V$, to that at constant pressure, $Q_P = \mathrm{R}(\partial[\ln\tau]/\partial(1/T))_P$, provides a quantitative measure of the relative importance of $T$ and $V$ on the dynamics. Both can be obtained from $T$- and $P$-dependent dielectric spectroscopy (DS) measurements. Recently, a correlation between the monomeric volume and the dynamic quantity $\mathscr{R}$ has been proposed[30] for a series of polymers and glass-forming liquids. Monomeric volume and local packing play a key role in controlling the value of this ratio and thus the dynamics associated with the glass temperature.

The purpose of the present investigation is 2-fold. First, to provide the canonical set of equations that describe the effect of the thermodynamic variables $P$, $V$, $T$ on the dynamics by deriving the corresponding equations. Second, with the aid of the dynamic ratio $\mathscr{R}$, to investigate the origin of the complex dynamics in poly (ethyl methacrylate) (PEMA). This polymer was chosen for this study because of its rich dynamics associated with the liquid-to-glass transformation ($\alpha$-process), the secondary relaxation ($\beta$-process), their coalescence to form the $\beta\alpha$-process, and a further, "slower", process that has not been discussed before. In particular, the $\alpha$-process, the $\beta$-process, their merging ("crossover") region, the merged $\beta\alpha$ and "slower" dynamic processes all occur within the extremely wide frequency, temperature and pressure window accessible by modern DS techniques. For this purpose we employ temperature- and pressure-dependent DS in combination with pressure-volume-temperature and rheology measurements on two PEMA samples with molecular weights of $2.0 \times 10^3$ and $1.59 \times 10^4$ g/mol. We discuss the four dynamic processes, $\alpha$, $\beta$, $\alpha\beta$, and "slow", and provide quantitative information on their origins through their pressure sensitivities (giving apparent activation volumes $\Delta V^{\#}$) and ratio $\mathscr{R}$ of activation energies. The dielectric studies reported here are a considerable extension and development of those made by Williams for PEMA.[4]

## II. Experimental Section

**Samples.** Two a-PEMA samples were employed in the present study, both prepared by radical polymerization with $M_w = 2.0 \times 10^3$ ($M_w/M_n \sim 1.2$) and $1.59 \times 10^4$ g/mol ($M_w/M_n \sim 1.6$). Molecular weights and polydispersities for the low and high molecular weight samples were determined by MALDI−TOF and SEC, respectively. The high molecular weight sample is identical to the one used in ref 17.

**Rheology.** An advanced rheometric system (ARES) equipped with a force-rebalanced transducer was used in the oscillatory mode. Depending on the sample and $T$-range, two transducers were used with 2000, 2 g·cm and 200, 0.2 g·cm upper and lower sensitivity, respectively. The samples were prepared on the lower plate of the 25 mm diameter parallel plate geometry setup and were heated under a nitrogen atmosphere until they could flow. Subsequently, the upper plate was brought into contact, the gap thickness was adjusted to 1 mm, and the sample was slowly cooled to the desired starting temperature. The storage ($G'$) and loss ($G''$) moduli were monitored in different types of experiments. First, the linear and nonlinear viscoelastic ranges were identified, by recording the strain amplitude dependence of the complex shear modulus $|G^*|$. These experiments involved (i) isochronal temperature scans aiming to identify the transition temperatures, (ii) isothermal frequency scans for temperatures in the range 323.15−383.15 K and for frequencies $10^{-2} < \omega < 10^2$ rad s$^{-1}$.

**Dielectric Spectroscopy.** The sample cell consisted of two electrodes, 20 mm in diameter and the sample with a thickness of 50 $\mu$m. The dielectric measurements were made at different temperatures in the range 133.15 to 453.15 K, at atmospheric pressure, and for frequencies in the range from $3 \times 10^{-3}$ to $1 \times 10^6$ Hz using a Novocontrol BDS system comprising a frequency response analyzer (Solartron Schlumberger FRA 1260) and a broadband dielectric converter with an active sample head. In addition, for the sample with $M_w = 2 \times 10^3$ g mol$^{-1}$, pressure-dependent measurements were made under "isothermal" conditions (the following temperatures were used: 353.15, 363.15, 373.15, 383.15, 393.15, 403.15, 413.15, 423.15 K) and for pressures in the range from 0.1 to 300 MPa. The complex dielectric permittivity $\varepsilon^* = \varepsilon' - i\varepsilon''$, where $\varepsilon'$ is the real and $\varepsilon''$ is the imaginary part, is a function of frequency $\omega$, temperature $T$, and pressure $P$, $\varepsilon^* = \varepsilon^*(\omega, T, P)$. In the analysis of the DS spectra we have used the empirical equation of Havriliak and Negami (HN)[31]

$$\varepsilon^*(T,P,\omega) = \varepsilon_\infty(T,P) + \frac{\Delta\varepsilon(T,P)}{[1 + (i\omega\tau_{HN}(T,P))^m]^n} + \frac{\sigma_0(T,P)}{i\varepsilon_f\omega} \quad (1)$$

where $\tau_{HN}(T,P)$ is the characteristic relaxation time, $\Delta\varepsilon(T,P) = \varepsilon_0(T,P) - \varepsilon_\infty(T,P)$ is the relaxation strength of the process under investigation, $m$, $n$ (with limits $0 < m$, $mn \leq 1$) describe, respectively, the symmetrical and asymmetrical broadening of the distribution of relaxation times, $\sigma_0$ is the dc-conductivity and $\varepsilon_f$ is the permittivity of free space. In the fitting procedure, we have used the $\varepsilon''$ values at every temperature and pressure and in some cases the $\varepsilon'$ data were also used as a consistency check. From $\tau_{HN}$, the relaxation time at maximum loss, $\tau_{max}$, is obtained analytically following:

$$\tau_{max} = \tau_{HN}\left[\frac{\sin\left(\frac{\pi m}{2+2n}\right)}{\sin\left(\frac{\pi mn}{2+2n}\right)}\right]^{-1/m} \quad (2)$$

In the temperature range where two relaxation processes ($\alpha$ and $\beta$) contribute to $\varepsilon^*$ there are two ways of representing the data.[12,7] The first one, followed here, is based on a summation of two HN functions and assumes statistical independence in the frequency domain. The second one, proposed by Williams and Watts[7] is a molecular theory, sometimes called the "Williams ansatz", for the dipole moment time-correlation function $C_\mu(t)$ (see Appendix). As discussed earlier, the relaxation times of the $\alpha$ and $\beta$-processes, thus determined, are nearly independent of the data evaluation method used.

Figure 1 shows some representative loss spectra for PEMA ($M_w = 2.0 \times 10^3$ g mol$^{-1}$) under "isobaric" (at 0.1 MPa) and "isothermal" (at 363.15 K) conditions. Decreasing

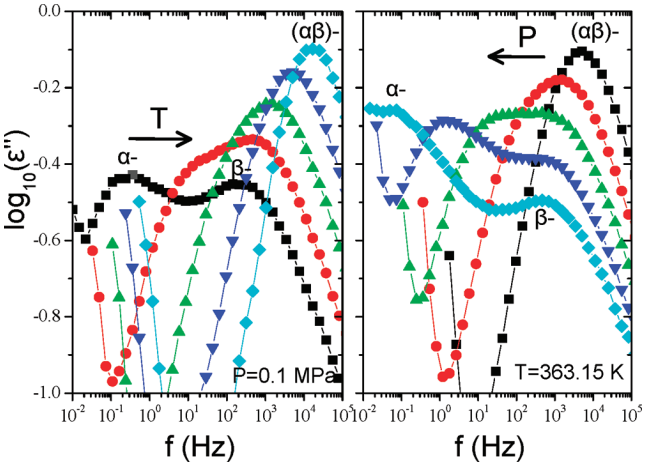


**Figure 1.** Dielectric loss curves for PEMA ($M_w = 2.0 \times 10^3$ g/mol) under "isobaric" ($P = 0.1$ MPa) (left) and "isothermal" (right) conditions ($T = 363.15$ K). The "isobaric" curves are at (squares): 333.15, (circles): 343.15, (up triangles): 353.15, (down triangles): 363.15, (rhombus): 373.15 K, and the "isothermal" curves at (squares): 0.1, (circles): 40, (up triangles): 80, (down triangles): 120 and (rhombus): 160 MPa. Notice the opposite effects of increasing $T$ and $P$ on the dynamics.

temperature and increasing pressure have the same effect qualitatively; both result in the demerging of the single ($\alpha\beta$)-process into two separate processes, $\alpha$ and $\beta$, as was first observed for PEMA by Williams[4] using more-limited ranges of temperature, pressure and frequency. As we will see below, pressure provides important information on the origins of the different processes that cannot be obtained by temperature variation alone.

An alternative representation of the dielectric data[32] is through the inverse of the dielectric permittivity $\varepsilon^*(\omega)$ i.e., the electric modulus, which is related to the dielectric permittivity through[1,31]

$$M^*(\omega) = \frac{1}{\varepsilon^*(\omega)} = M' + iM'' \tag{3}$$

where $M'$ and $M''$ are the real and imaginary parts of the electric modulus, respectively. The electric modulus representation (i.e., the decay of the electric field under conditions of constant dielectric displacement, $D$) rather than the complex permittivity (constant electric field, $E$) has been proposed not only for systems containing a substantial concentration of mobile carriers but also for any dielectrically active process. There are also cases where the use of $M^*(\omega)$ is an absolute necessity (i.e., for comparison with rheology data). The relaxation times obtained from the electric modulus ($\tau_{M^*}$) and the complex permittivity ($\tau_{\varepsilon^*}$) representations scale[1] as $\tau_{M^*}/\tau_{\varepsilon^*} \sim \varepsilon_\infty/\varepsilon_s$ (exact equality applies only for the case of $m = n = 1$) and can differ substantially in systems with high dielectric strengths. On the other hand, in systems with weak dielectric processes the two relaxation times are nearly equal.

**Pressure−Volume−Temperature.** Literature values were used for the $PVT$ equation of state.[33] The Tait equation of state was employed

$$V(P,T) = V(0,T)\left\{1 - 0.0894 \ln\left[1 + \frac{P}{B(T)}\right]\right\} \tag{4}$$

where for $T < T_g$, the specific volume at atmospheric pressure was $V(0,T) = 0.889 + 2.1 \times 10^{-4} T + 1.32 \times 10^{-7} T^2$ ($V$ in cm$^3$/g, $T$ in °C) and $B(T) = (294.0 \text{ MPa}) \exp(-0.0041T)$ ($T$ in °C), while at $T > T_g$, $V(0,T) = 0.847 + 9.5 \times 10^{-4} T + 6.6 \times 10^{-7} T^2$ ($V$ in cm$^3$/g, $T$ in °C) and $B(T) = (238.0 \text{ MPa}) \exp(-0.0054T)$ ($T$ in °C).

## III. Theoretical Section

**Derivation of the Ratio of Activation Energies.** A critical test of the origin of the different processes and of the relative influence of volume and temperature in each case is provided by the value of the ratio $\mathscr{R}$ of the apparent activation energy at constant volume, $Q_V(T,V)$, to that at constant pressure, $Q_P(T,P)$[3−7,29]

$$\mathscr{R} = (\partial[\ln \tau]/\partial(1/T)_V)/(\partial[\ln \tau]/\partial(1/T)_P) = Q_V(T,V)/Q_P(T,P)$$

$\mathscr{R}$ assumes values in the range $0 \le \mathscr{R} < 1$ and provides a quantitative measure of the role of temperature and density on the dynamics. Values near unity suggest that the dynamics are governed mainly by the thermal energy whereas values near zero suggest that free volume ideas prevail, since in that case, $Q_V = 0$. However, no polymer or glass-forming liquid has the extreme values of 0 or 1 for $\mathscr{R}$, suggesting that the picture is more complicated than the two extreme cases considered above.[23,30]

Herein the effects of $(T,P,V)$ on a relaxation time $\tau$ are considered together in *one theoretical framework*. Note that along with $T$ and $P$ as intensive variables, we ensure that $V$ is also an intensive variable by defining it as "specific volume" (m$^3$ kg$^{-1}$). We form the ratios $(\partial \ln \tau/\partial W)_X/(\partial \ln \tau/\partial Y)_Z$ where $(W,X,Y,Z)$ are permutations of $(V,T,P)$. For brevity and convenience we employ a compact notation $(\partial[\ln \tau]/\partial W)_X = WX$ that uses only the subscripts $WX$, so the required ratios are given by

$$(\partial[\ln \tau]/\partial W)_X/(\partial[\ln \tau]/\partial Y)_Z = WX/YZ \tag{5}$$

Writing $\tau = \tau(T,P)$ and $V = V(T,P)$, there are thirty six possible ratios $WX/YZ$. We seek those ratios that allow $(WX/YZ)$ to be related to $\mathscr{R}$ and certain thermodynamic properties for a material. The six special cases $WX/WX$, e.g., $PT/PT$, are all unity so are discarded. A total of 12 ratios of the form $YZ/WX$, where $X \neq Z$ are reciprocals of $WX/YZ$, thus are eliminated, while three ratios of the form $WX/YX$ are reciprocals of $YX/WX$ and are also eliminated. This leaves 15 ratios to be determined. Each ratio can be expressed as functions of $\mathscr{R}$ and the isobaric expansion coefficient $\alpha_P = (\partial \ln V/\partial T)_P$, the isothermal compressibility $\beta_T = -(\partial \ln V/\partial P)_T$, and the thermal pressure coefficient $(\partial P/\partial T)_V = \alpha_P/\beta_T$. There are different routes to obtain these ratios so, for convenience to a reader, details of the derivations are given in the Supporting Information. Ratios with $W \equiv Y$, $X \neq Z$

$$VP/VT = (\partial[\ln \tau]/\partial V)_P/(\partial[\ln \tau]/\partial V)_T = (1-\mathscr{R})^{-1} = 1-(\partial V/\partial T)_\tau/(\partial V/\partial T)_P \tag{6}$$

$$TV/TP = (\partial[\ln \tau]/\partial T)_V/(\partial[\ln \tau]/\partial T)_P = \mathscr{R} = 1-(\partial T/\partial P)_\tau/(\partial T/\partial P)_V = (\partial V/\partial P)_\tau/(\partial V/\partial P)_T \tag{7}$$

$$PV/PT = (\partial[\ln \tau]/\partial P)_V/(\partial[\ln \tau]/\partial P)_T = -\mathscr{R}(1-\mathscr{R})^{-1} = 1-(\partial P/\partial T)_\tau/(\partial P/\partial T)_V \tag{8}$$

Ratios with $W = Z$, $X = Y$

$$TV/VT = \mathscr{R}(1-\mathscr{R})^{-1}(\partial V/\partial T)_P = -(\partial V/\partial T)_\tau \quad (9)$$

$$PV/VP = -\mathscr{R}(\partial V/\partial P)_T = -(\partial V/\partial P)_\tau \quad (10)$$

$$PT/TP = -(1-\mathscr{R})/(\partial P/\partial T)_V = -(\partial T/\partial P)_\tau \quad (11)$$

Ratios with $W = Z$, $X \neq Y$

$$TP/VT = (1-\mathscr{R})^{-1}(\partial V/\partial T)_P \quad (12)$$

$$TV/PT = -\mathscr{R}(1-\mathscr{R})^{-1}(\partial P/\partial T)_V \quad (13)$$

$$PT/VP = (1-\mathscr{R})(\partial V/\partial P)_T \quad (14)$$

$$PV/TP = \mathscr{R}/(\partial P/\partial T)_V \quad (15)$$

$$VP/TV = \mathscr{R}^{-1}/(\partial V/\partial T)_P \quad (16)$$

$$VT/PV = -\mathscr{R}^{-1}(1-\mathscr{R})/(\partial V/\partial P)_T \quad (17)$$

Ratios with $W \neq Z$, $X \neq Y$

$$TV/PV = (\partial P/\partial T)_V \quad (18)$$

$$VP/TP = 1/(\partial V/\partial T)_P \quad (19)$$

$$PT/VT = (\partial V/\partial P)_T \quad (20)$$

Equations 6−20 apply to a system where the thermodynamic properties do not change within the time-scale of the measurements. This is the case for a material above $T_g$, where the system is strictly ergodic, and below $T_g$ where the glass, although a nonergodic system, has thermodynamic and relaxation properties (of the kind studied here) which are determined by the thermal/pressure/time "path" used for its preparation.

Equations 6−20 give a unified scheme for the variations of $\tau$ with respect to $(T,P,V)$. Two approaches may be used to determine $\mathscr{R}$ from eqs 6−11. For eq 6−8, a ratio $WX/YZ$ is determined experimentally and $\mathscr{R}$ follows directly: e.g. $PV/PT$ with eq 8. For eq 9−17 a ratio $WX/YZ$ is determined experimentally and $\mathscr{R}$ follows with the aid of $\alpha_P$, $\beta_T$ or $(\alpha_P/\beta_T)$: e.g. $PT/TP$ with $(\partial P/\partial T)_V$ and eq 11. Alternatively, for eq 6−11 a ratio $(\partial W/\partial X)_\tau$ is determined experimentally, where $(W,X)$ are permutations of $(T,P,V)$, then $\mathscr{R}$ follows with the aid of $\alpha_P$, $\beta_T$ or $(\alpha_P/\beta_T)$: e.g., $(\partial T/\partial P)_\tau$ and $(\partial P/\partial T)_V$ with eq 11. In this example, plots of ln $\tau$ vs $P$ at constant values of $T$ yield plots of $T$ vs $P$ for constant values of$\tau$, allowing $(\partial T/\partial P)_\tau$to be determined. If $\tau$ is chosen to be that at the apparent glass transition temperature $T_g$ of the material (normally taken to be $10^2$ s) then this is sometimes termed $dT_g/dP$, representing the variation of $T_g$ with applied pressure. In the original work of Williams[3b] in 1964 for the dielectric α-process in PMA, $\mathscr{R}$ was derived and written in the alternative forms

$$TV/TP = 1-[RT^2/Q_P(T,P)][(\partial[\ln\tau]/\partial P)_T](\partial P/\partial T)_V \quad (21a)$$

$$TV/TP = 1-[(\partial P/\partial T)_V/(\partial P/\partial T)_\tau] \quad (21b)$$

These are equivalent to eq 7 above. In the original work[3b] $Q_V(T,V)$ was determined using eq 21a, allowing $\mathscr{R}$ to be determined, while plots of $T$ vs $P$ at constant $\tau$ were constructed to give $(\partial T/\partial P)_\tau$.

Further equations are derived in the Supporting Information, and yield

$$\mathscr{R} = A[1+\lambda_a]^{-1} = [1+\lambda_b/A]^{-1} = \mathscr{R} = [1+\lambda_c/A]^{-1} \quad (22)$$

$$A = 1-T(\partial[\ln Q]/\partial T)_V, \quad \lambda_a = -T(\partial[\ln Q]/\partial T)_P,$$
$$\lambda_b = T(\partial[\ln Q]/\partial P)_T(\partial P/\partial T)_V,$$
$$\lambda_c = -T(\partial[\ln Q]/\partial V)_T(\partial V/\partial T)_P \quad (23a-d)$$

For the special case where (i) $Q$ is a function of $V$ only, i.e., $Q = Q(V)$, and (ii) takes the form $Q = C/V^\gamma$, as proposed by Roland and co-workers,[34,35] where $C$ and $\gamma$ are material constants, it follows that $\mathscr{R} = (1 + T\gamma\alpha_P)^{-1}$, in which case $\mathscr{R}$ decreases with increasing temperature.

In 1964, Williams[3a] derived an extension of the Eyring transition state theory for chemical reactions for application to structural relaxation in polymers that gave the following equations

$$-RT^2(\partial[\ln\tau]/\partial T)_P = \Delta H^\#(T,P) + RT/2$$
$$-RT^2(\partial[\ln\tau]/\partial T)_V = \Delta E^\#(T,V) + RT/2$$
$$(\partial[\ln\tau]/\partial P)_T = \Delta V^\#(T,P)/RT \quad (24a,b,c)$$

where $\Delta H^\#$, $\Delta E^\#$, and $\Delta V^\#$ are, respectively, the "activation enthalpy", "activation internal energy" and "activation volume", defined with respect to unactivated and activated standard states of a relaxor.[3a] This analysis has been further discussed in several papers (see refs 36−38 and refs therein), with a special consideration of the standard states being given by Albuquerque and Reis[37,38] in their comprehensive thermodynamic formalism for the constant volume principle as applied to chemical reactions and molecular relaxation processes.

Naoki et al.[29] used eq 11 subsequently to determine $\mathscr{R}$ for the dielectric α-process in *o*-terphenyl, while Roland and co-workers[34,35] used eq 7 and the special case above for the same process in glass-forming liquids and amorphous polymers. On the other hand, Floudas et al.[39,40] employed eq 6 for amorphous polymers. Hoffman, Williams, and Passaglia[41] used the fact that $\mathscr{R}$ values for the dielectric α-relaxation in amorphous polymers were fairly large ($>0.65$) to conclude that the simple free volume theories of the glass transition[28] were incorrect (see below), an important observation that has been overlooked in polymer science over the intervening years. Subsequently, Floudas et al.[30] have shown that the repeat unit volume and local packing play a key role in controlling the value of this ratio at $T_g$, and thus the dynamics associated with the glass temperature. In particular, for *flexible* main-chain polymers, temperature, through

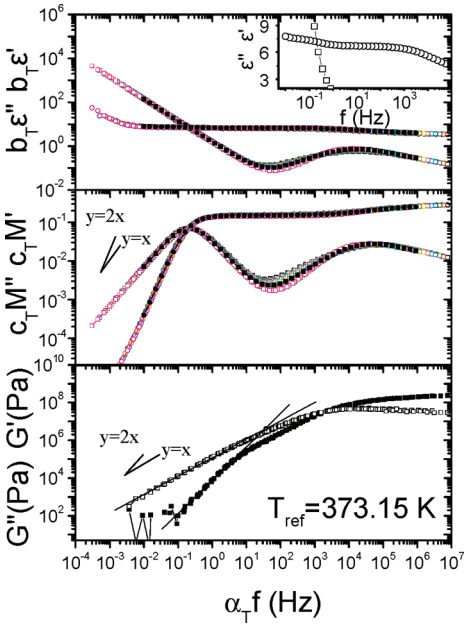


**Figure 2.** Comparison of the complex dielectric function ($\varepsilon^*$), the electric modulus ($M^*$) and the viscoelastic (shear) moduli ($G^*$) of PEMA ($M_w = 2.0 \times 10^3$ g/mol), at the same reference temperature ($T_{ref} = 373.15$ K). Top: Master curve construction using the principle of time−Temperature superposition ($t$Ts) for the "isobaric" (at $P = 0.1$ MPa) dielectric permittivity (circles) and the dielectric loss (squares) data of $\varepsilon^*$. The filled symbols correspond to the measurement at the reference temperature. In the inset the dielectric permittivity (circles) and the dielectric loss (squares) curves are shown at $T = 373.15$ K. Middle: Master curve construction using $t$Ts for the "isobaric" (at $P = 0.1$ MPa) electric modulus data of the real (circles) and imaginary (squares) part of $M^*$. Bottom: Master curve construction for the storage (filled squares) and loss (open squares) shear moduli ($G^*$) of PEMA. Lines with slopes 1 and 2 are drawn, and the range used to define the terminal relaxation times is shown.

the presence of energy barriers opposing molecular motions, is the main parameter affecting the dynamics whereas in polymers with *bulky side groups* or in glass-forming liquids with large molar volumes, volume effects gain importance. A similar conclusion was reached by a recent theory of glass formation[42] whereas another method emphasized the importance of intermolecular cooperativity of motions (and fragility).[43]

## IV. Experimental Results and Discussion

**Temperature Dependence of Relaxation Times.** The components of the dielectric function ($\varepsilon'$ and $\varepsilon''$) and the corresponding electric modulus ($M'$ and $M''$), measured within the temperature range: $357.15 \le T \le 403.15$ K, are compared in Figure 2, at the same (reference) temperature, $T_r = 373.15$ K, for the sample with $M_w = 2.0 \times 10^3$ g/mol. In the Figure, the frequency axes have been multiplied by appropriate shift factors ($\alpha_T$) at each $T$ in order to bring the low-frequency maxima of $M''$ (corresponding to the ionic mobility process) into coincidence with $M''_{max}$ at the reference temperature (373.15 K). The vertical axes have also been shifted slightly by shift factors $b_T$ (for $\varepsilon^*$) and $c_T$ (for $M^*$). In the inset to the $\varepsilon^*$ representation, the $\varepsilon'$ and $\varepsilon''$ data at 373.15 K are plotted in the region of their crossing. The dispersion of $\varepsilon'$ at low frequencies seen in the inset signifies there is a relaxation process associated with the ionic mobility process and this is confirmed by the ($M'$,$M''$) data in Figure 2. The superposition of the latter data to form a "master curve" indicates that time−temperature superposition ($t$Ts) works well for the ionic mobility process. However, for the peak in $c_T M''$ (and $b_T \varepsilon''$), which is due to dipole relaxation, $t$Ts fails on the low frequency side because it has a complex structure due to the presence of

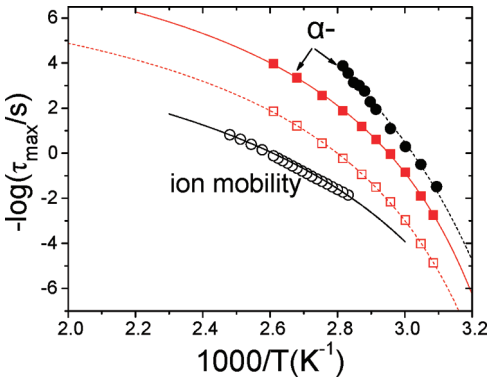


**Figure 3.** Arrhenius representation of the segmental and terminal relaxation times of PEMA ($M_w = 2.0 \times 10^3$ g/mol). The DS relaxation times are shown for the α-process (filled circles) and for the process due to the ionic mobility (open circles). The rheology segmental (filled squares) and terminal (open squares) times are shown for the same sample. The lines are fits to the VFT equation.

α-, $\beta$- and α$\beta$-processes, which have different temperature dependencies.

In Figure 2, the shifted curves from the shear moduli data (measured in the temperature range $324.15 \le T \le 383.15$ K and shifted horizontally with the same shift factors as for the $\varepsilon^*$ and $M^*$ representations) are shown at the same reference temperature (373.15 K). Notice that the $t$Ts for the rheology data works reasonably well over the whole range, in contrast to its failure in the $\varepsilon^*$ and $M^*$ representations, where the temperature/frequency range investigated is much broader and separation into component dielectric processes is evident (see Figure 1(left)). Furthermore, in Figure 2c, the absence of a low frequency plateau in $G'$ and the proximity of the segmental and terminal relaxations (the latter being obtained from the crossing of the lines with slopes 1 and 2, for the $G''$ and $G'$ data, respectively) is a consequence of the low molecular weight of this sample.

In Figure 3, dielectric relaxation times, determined from $M''$ data (circles), for processes associated with segmental and ion mobility are compared with the segmental and terminal relaxations from rheology data (squares). The segmental and ion mobility processes (the latter with Havriliak−Negami shape parameters of $m = 0.98 \pm 0.01$, $n = 0.88 \pm 0.05$ for $M''(f)$ as obtained from DS, display the usual strong $\tau(T)$ dependence according to the Vogel−Fulcher−Tammann (VFT) equation

$$\tau_{max} = \tau_0 \exp\left(\frac{D_T T_0}{T - T_0}\right) \qquad (25)$$

where $D_T$ is a dimensionless parameter and $T_0$ is the "ideal" glass temperature located below $T_g$. The VFT parameters for the segmental and ion mobility processes as well as the segmental and terminal relaxations investigated by rheology are summarized in Table 1 where the corresponding VFT parameters for the ($\beta\alpha$)-process are also shown (the latter with Havriliak−Negami shape parameters of $m = 0.70 \pm 0.10$, $n = 0.55 \pm 0.10$ for $\varepsilon''(f)$ and $m = 0.65 \pm 0.10$, $n = 0.45 \pm 0.10$ for $M''(f)$). The comparison shows that the α-process obtained from DS is about 1 decade faster than the corresponding process obtained from rheology. A similar difference for the segmental processes was also obtained in ref 17. A comparison between the slow dielectric process and the terminal process obtained by rheology, revealed that the dielectric process associated with the ion mobility is about two decades slower. This implies that ionic mobility is decoupled from the longest chain relaxation (flow). To further explore the slow dielectric process we have undertaken annealing experiments at different temperatures above $T_g$ ($T = T_g + 60$ K) for different time intervals in 12 h steps. These experiments revealed decreasing amplitude with annealing time as in bisphenol A-polycarbonate[40] in contrast to that for the

**Table 1. Vogel−Fulcher−Tammann Parameters of the Relaxation Processes in PEMA ($M_w$ = 2.0 × $10^3$ g/mol and 1.59 × $10^4$ g/mol) at $P$ = 0.1 MPa**

| MW (g/mol) | method | process | $\tau_0$ (s) | $D_T$ | $T_0$ (K) | $T_g$ (K)[a] |
|---|---|---|---|---|---|---|
| 2000 | DS | ion mobility | $8.8 \times 10^{-7}$ | 6.9 ± 0.1 | 256 ± 2 | |
| | | α- | $5.7 \times 10^{-15}$ | 10.7 ± 0.2 | 254 ± 1 | 322 ± 1 |
| | | (αβ)- | $4.0 \times 10^{-15}$ | 27.8 ± 0.2 | 166 ± 3 | |
| | rheology | terminal | $1.5 \times 10^{-8}$ | 5.8 ± 0.1 | 271 ± 1 | |
| | | α- | $1.1 \times 10^{-10}$ | 5.8 ± 0.1 | 271 ± 1 | 340 ± 1 |
| 15900 | DS | ion mobility | $6 \times 10^{-6}$ | 8.0 ± 0.1 | 235 ± 2 | |
| | | α- | $5.3 \times 10^{-16}$ | 10.7 ± 0.1 | 264 ± 1 | 334 ± 1 |
| | | (αβ)- | $9.4 \times 10^{-15}$ | 27.8 ± 0.2 | 166 ± 3 | |

[a] $\tau = 10^2$ s.

segmental process, implying that ion mobility is coupled to stress relaxation.

Recently, advanced NMR techniques[16−18] revealed extended backbone chain conformations, with conformational memory, as the molecular units involved in structural relaxation of poly(*n*-alkylmethacrylates). These extended backbone conformation gave rise to a dynamic process that was longer than the fast axial reorientation associated with the dielectric α- and αβ-processes. Thus the origin of the motion was the randomization/isotropization of extended chain segments, comprising 5−10 repeat units that is promoted by the local structure in poly(*n*-alkylmethacrylates). Nevertheless, this process is faster than the complete chain relaxation as measured by rheology and hence by the even slower process due to the ionic mobility.

**Molecular Weight Dependence.** The four dielectrically active processes (α, β, αβ, and "slow") of PEMA for the two molecular weights (filled and open symbols corresponding to the low and high molecular weights, respectively), observed at ambient pressure, are compared in Figure 4, in the usual Arrhenius representation. The relaxation times were determined from HN-fits to dielectric loss data as those in Figure 1.

Figure 4 shows the β-process has an Arrhenius $T$-dependence,$\tau_{max} = \tau_0 \exp(Q_P/RT)$, where $\tau_0$ (~1.4 × $10^{-15}$ s) is the relaxation time limit at very high temperatures and $Q_P$ (~ 80 kJ $mol^{-1}$) is the constant pressure activation energy. The corresponding Havriliak−Negami shape parameters for this process are $m = 0.42 \pm 0.08$, $n = 0.85 \pm 0.08$ for $M''(f)$. The frequency−temperature locations of the β-process depend only slightly on the molecular weight in accord with the local character of the motion. The dielectric β-process arises from the motions of the dipolar side-chains in PEMA. A β-process observed in NMR studies of PEMA[16−18] involve π flips around the C−C backbone bond coupled with a restricted rocking motion of the backbone around its local extended chain axis, but it is not clear if such motions would lead to a relaxation strength for the dielectric β-process comparable to that observed here, or with such a broad apparent distribution of relaxation times. At longer times the α-process takes over, reflecting the fast axial reorientation of chain segments (NMR). At a certain temperature (here called $T_x$), the α- and β-processes merge to a single (αβ)-process. The (αβ)-process relaxes with a rate intermediate to the extrapolated rates from the α- and β-processes to $T > T_x$. The presence of a single, broad dynamic process at high temperatures suggests that the (αβ)-process is a distinct and separate process as proposed earlier.[4] The exact origin of the process and the extent of intra- and intermolecular contributions will be discussed below with respect to the pressure dependence.

As we can see in Figure 4, the characteristic temperature $T_x$, moves to higher frequencies/temperatures with increasing molecular weight (i.e., from $T_{x,(2000\ g/mol)} \sim 357$ K to

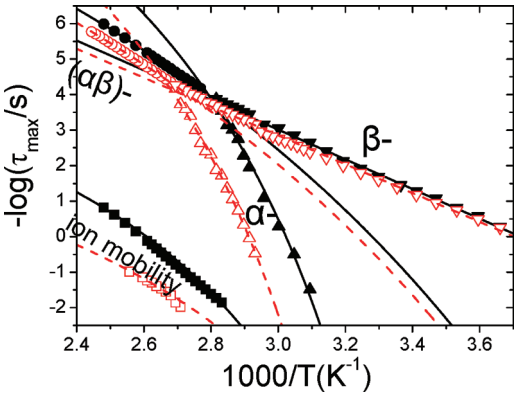


**Figure 4.** Temperature dependence of the relaxation times at maximum loss for the processes observed in PEMA where the filled symbols correspond to the low molecular weight sample ($M_w$ = 2.0 × $10^3$ g/mol) and the open symbols correspond to the high molecular weight sample ($M_w$ = 1.59 × $10^4$ g/mol). At higher temperatures the process due to the ion motion (squares) and the (αβ)- (circles) relaxation are shown, while at lower temperatures the α- (up triangles) and β- (down triangles) processes are shown. The lines are fits to the VFT equation for the slow, (αβ)- and α-processes, and to the Arrhenius equation for the β-process. Notice the higher splitting temperature, $T_x$, for the higher molecular weight sample as a result of the stronger molecular weight dependence of the segmental process.

$T_{x,(15900\ g/mol)}$~374 K). This is due to the stronger molecular weight dependence of the α-process as compared to the β-process. At even longer times the process due to the ionic mobility dominates the dielectric response. Interestingly, the ion motion is sensitive to the local segmental friction as indicated in Figure 4. The VFT parameters for the slow, (αβ)- and α-processes are summarized in Table 1. As for the uncertainty of the extracted times, in the case of the separated α-, β-, and αβ-processes is provided by the symbol size. In the vicinity of $T_x$ (for $T \sim T_x \pm 10$ K), the α- and β-processes approach and finally merge and, in this case, the uncertainty of relaxation times may slightly exceed the symbol size.

**Pressure Dependence.** The origins of the merged (αβ)-process and its relation to the separate α- and β-processes can best be studied by combining $T$- with $P$-dependent relaxation studies. For this purpose we employ the PEMA sample with $M_w$ = 2.0 × $10^3$ g/mol and carry our "isothermal" measurements as a function of pressure for several different temperatures. Consider first the effects of pressure on the relaxation intensities of the different processes. With respect to Figure 1, the (αβ)-process "demerges" with increasing pressure to form α- and β-processes. Notice that the spectra taken under near "isochronal" conditions (i.e., data at $P$ = 0.1 MPa, $T$ = 333.15 K and $T$ = 363.15 K, $P$ = 80 MPa) differ in the relative intensities for the α- and β-processes. Pressure results in the densification of dipoles, but that would increase the relaxation strength of both processes

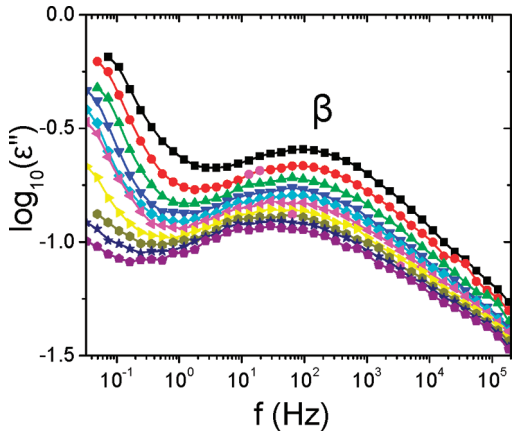


**Figure 5.** Dielectric loss curves for PEMA ($M_w$ = 2.0 × $10^3$ g/mol) under "isothermal" conditions at $T$ = 323.15 K corresponding to the $\beta$-process. The curves are at (squares): 0.1, (circles): 30, (up triangles): 60, (down triangles): 90, (rhombus): 120, (left triangles): 150, (right triangles): 180, (polygons): 210, (stars): 240, and (pentagons): 270 MPa.

by only a few percent. The changes in relative intensity of the α- and $\beta$- processes in the figures are far greater than this and give important information on the nature of each process. The behavior in Figure 1 (right) is observed at other temperatures (see Supporting Information). In all cases the marked decrease in $\beta$-relaxation strength $\Delta\varepsilon_\beta$ with increasing pressure is accompanied by a complementary increase in $\Delta\varepsilon_\alpha$. This may be explained by the concept of partial and total relaxations (see the Appendix). The case of PEMA is particularly interesting since the relaxation of the dipole moment $\mu$ of the chain repeat unit occurs by reorientations of the ester side groups, that relax only a part of $\langle\mu^2\rangle$, giving the $\beta$-process, and motions of the chain backbone (α-process) that relax the remainder of $\langle\mu^2\rangle$. This gives rise to the pattern of α-, $\beta$-, and α$\beta$-processes observed here for this polymer, and to their behavior with respect to variations in sample temperature and applied pressure. As noted there, for reasons to be determined, increased pressure decreases the spatial extent of the motions of the dipole moment $\mu_s$ of the ester side chains, giving a decrease in $\Delta\varepsilon_\beta$ and an increase in $\Delta\varepsilon_\alpha$ in order to conserve the total relaxation strength. Plots of $\Delta\varepsilon_\alpha$, $\Delta\varepsilon_\beta$, and $\Delta\varepsilon_{\beta\alpha}$ vs pressure for different temperatures are shown in the Supporting Information. Figure 5 provides the effect of pressure on the glassy state dynamics.

It is noted that at ($T$ = 323.15 K, $P$ = 0.1 MPa) the α-process has moved to ultralow frequencies, yet, as was also seen by Williams,[4] there is still a very large effect of pressure on $\Delta\varepsilon_\beta$. Thus, although changes in the average relaxation time and line-shape are minor with increasing pressure, there is a major reduction in the dielectric strength of the $\beta$-process showing that compression has a large effect on the extent of motions of the side-chain dipoles even in the glassy state. The fact that the $\beta$-process loses intensity on pressurization, may reflect the "blocking" of this motion as proposed by Heijboer.[44]

Representative relaxation maps under both "isothermal" and "isobaric" conditions are shown in Figure 6 for this material.

For the "isobaric" data (left) the lines correspond to fits according the VFT equation for the ion, (α$\beta$)-process and α-processes and to the Arrhenius equation for the $\beta$-process. For the "isothermal" data (right), the $\beta$- and (α$\beta$)-process were adequately described by a linear dependence, whereas for the α-process use of the modified VFT equation for pressure is a necessity,[45]

$$\tau_{max} = \tau_\alpha \exp\left(\frac{D_P P}{P_0 - P}\right) \quad (26)$$

In the equation above, $\tau_\alpha$ is the segmental relaxation time at atmospheric pressure at a given temperature, $D_P$ is a dimensionless parameter and $P_0$ is the pressure corresponding to the ideal glass transition. Clearly $(\partial[\log\tau]/\partial P)_T$ values for the α-, (α$\beta$)- and the ion process are considerably larger than that for the $\beta$-process (we will discuss this observation below, with respect to the apparent activation volume and ratio of activation energies).

Next we focus on the "isotherms" of Figure 6, and we discuss the effect of pressure on the separation of the mixed (α$\beta$)-process. At temperatures above $T_x$, (at atmospheric pressure) only the coalesced ($\beta$α-process) is observed (at high frequencies) which slows down with increasing pressure. At a certain pressure ($P_x$) the (α$\beta$)-process separates into α- and $\beta$-processes.

This pressure has a temperature dependence that is depicted in Figure 7 (noted as "splitting line") according to $T_x$ = 363.6 + 0.25 × $P_x$, $T_x$ in K, $P_x$ in MPa. In the same figure, the extrapolated glass temperatures (obtained at $\tau \sim$ 100 s) from the α-process, the slower processes associated with the freezing of the ion mobility, and of the merged (α$\beta$)-process are plotted. We mention here that the $T_g(P)$ data corresponding to the latter process should be taken only as indicative as they result from an extrapolation from over 6 decades (see Figure 6). In Figure 7, the lines are fits to the "isothermal" and "isobaric" data points corresponding to the α-, (α$\beta$)-, and ion mobility processes according to the empirical equation,

$$T_g(P) = T_g(0)\left(1 + \frac{\kappa}{\lambda}P\right)^{1/\kappa} \quad (27)$$

first proposed by Simon and Glatzel[46] for the melting of solidified gases under pressure and subsequently employed by Andersson and Andersson[47] and others[39,40,48] to describe the $T_g(P)$ of glass-forming systems. In the above equation, $T_g(0)$ is the temperature (at $P$ = 0.1 MPa) where the characteristic relaxation time of each process corresponds to 100 s, and $\kappa$, $\lambda$ are polymer specific parameters (the parameters are summarized in Table 2, where the values of the initial slopes $(dT/dP)_{P\to 0}$ are also given).

The initial slopes of the "isothermal" lines of Figure 6 (right part), result in the apparent activation volume, $\Delta V^\#$ using eq 24. This quantity is plotted in Figure 8 as a function of temperature for all processes investigated. In extracting $\Delta V^\#$, we have used the single-valued slopes for the $\beta$-process whereas the initial slopes (i.e., at applied pressure $P\to 0$) were used for the remaining processes.

The apparent activation volume of the α-process shows the expected temperature dependence from a number of amorphous polymers investigated so far.[23,24,39,40,48,49] At high temperatures, $\Delta V^\#$, approaches the monomer volume of PEMA ($V_m$ = 102 $cm^3$/mol), while at lower temperatures ($T \sim T_g$), it increases dramatically. On the contrary, the corresponding quantity for the $\beta$-process is temperature independent with its value being only a fraction of the monomer volume. The values of the apparent activation volume for the (α$\beta$)-process and ion mobility process are similar, with their values being in the proximity of the monomer volume. Furthermore they display some $T$-dependence as with the α-process. The proximity of $\Delta V^\#$ values for

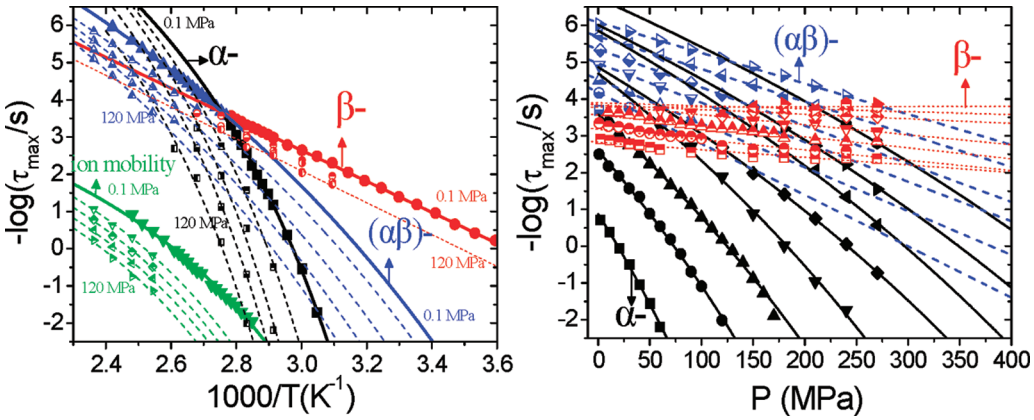


**Figure 6.** Left: Arrhenius representation of the relaxation times at maximum loss for the processes (α-, $\beta$-, ($\alpha\beta$)- and ion mobility as indicated) for PEMA ($M_w = 2.0 \times 10^3$ g/mol) and for pressures in the range of $0.1 < P < 120.0$ MPa plotted in 30.0 MPa steps. The lines are fits to the VFT equation for the slow, ($\alpha\beta$)- and α-processes and to the Arrhenius equation for the $\beta$-process. Right: Pressure dependence of the relaxation times at maximum loss for the ($\alpha\beta$)-, α- and the $\beta$-process of PEMA ($M_w = 2.0 \times 10^3$ g/mol) for temperatures in the range of $353.15 < T < 423.15$ K, in steps of 10 K. The lines are fits to the pressure modified VFT equation for the α-process whereas linear fits are made for the $\beta$- and ($\alpha\beta$)-processes.

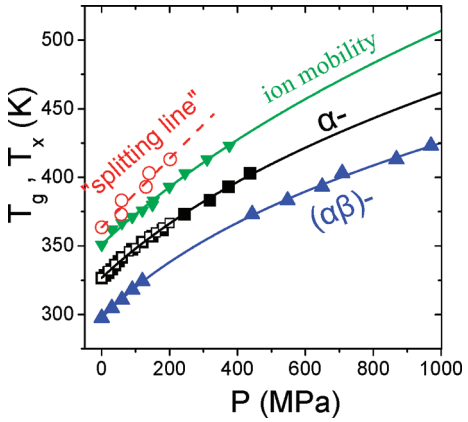


**Figure 7.** $T(P)$ representation of PEMA ($M_w = 2.0 \times 10^3$ g/mol). (open squares): $T_g$ obtained from PVT measurements; (filled squares): $T_g$ and $P_g$ obtained from "isobaric" and "isothermal" DS relaxation times, respectively ($T_g$ is operationally defined here as the temperature where the segmental relaxation time is at 100 s); (down triangles): obtained from "isobaric" and "isothermal" DS relaxation times respectively for the ion mobility process (at $\tau \sim 100$ s). The up triangles correspond to the ($\alpha\beta$)-process, but we mention that these "phenomenological" data originate from an extrapolation over almost 6 decades (see Figure 6). On the same diagram the pressure dependence of the splitting temperature is plotted with open circles. The curves are fits to an empirical equation for the ionic mobility, ($\alpha\beta$)- and α-processes (see Table 2). The "splitting line" data were fitted according to $T_x = 363.6 + 0.25 \times P_x$ ($T_x$ in K and $P_x$ in MPa).

the ($\alpha\beta$)-process to the α-process rather than to the local $\beta$-process, confirms that the process is due to segmental relaxation. The main chains move in segmental motions (α-process), facilitated by local motions of the side chains, so carry with them the dipole moment components $\mu_b$ and $\mu_s$ of the ester side chains in one overall motion ($\alpha\beta$-process) thus relaxing all of $\langle\mu^2\rangle$ (see Appendix). We will return to this point later in the discussion of the dynamic ratio.

A more critical test of the origin of the different relaxation processes in PEMA can be provided by the value of $\mathcal{R} = Q_V(T,V)/Q_P(T,P)$ which, for the transition state theory, ignoring the small term $RT/2$, corresponds to $\Delta E^{\#}/\Delta H^{\#}$ (see eq 24 above). Experimentally this ratio can also be obtained, for each of the relaxation processes, from the $\tau(\rho)$ representation using eq 6. This is made by coupling the relaxation times measured under "isobaric" $\tau(T)$ and "isothermal" $\tau(P)$ conditions with the equation of state $V(T,P)$. The results for the dielectric processes observed in

**Table 2. Parameters of Equation 27 and Initial Slopes $(dT/dP)_{P\to 0}$ for PEMA with $M_w = 2.0 \times 10^3$ g/mol**

| process | $T_g(0)^a$ (K) | $\lambda$ (MPa) | $\kappa$ | $(dT/dP)_{P\to 0}$ (K/MPa) |
|---|---|---|---|---|
| α- | 327 ± 1 | 1396 ± 22 | 3.8 ± 0.1 | 0.234 |
| ion mobility | 351 ± 1 | 1448 ± 15 | 3.0 ± 0.1 | 0.242 |
| ($\alpha\beta$)- | 298 ± 1 | 1171 ± 20 | 4.4 ± 0.2 | 0.254 |
| splitting | 333 ± 3 | | | 0.250 |

$^a$ At $\tau = 10^2$ s.

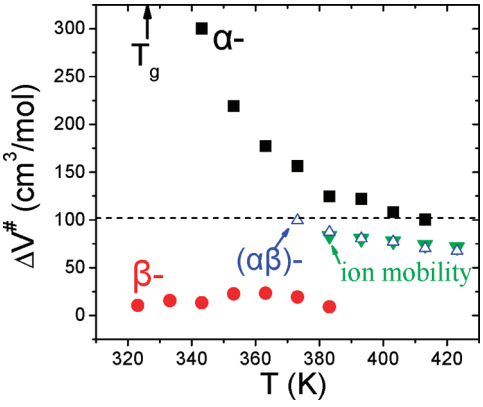


**Figure 8.** Apparent activation volume, $\Delta V^{\#}$, as a function of temperature for the α- (filled squares) the ($\alpha\beta$)- (open up triangles) the $\beta$- (filled circles), and the ion mobility (filled down triangles) processes of PEMA ($M_w = 2.0 \times 10^3$ g/mol). The horizontal line gives the monomer volume ($V_m = 102$ cm$^3$/mol).

PEMA are shown in Figure S3 (Supporting Information). The solid and dashed lines represent the "isothermal" and "isobaric" pathways in the $\tau(\rho)$ representation and the lines are fits to the modified VFT equation for the density representation,[23,24,39,40,48,49]

$$\tau_{max} = \tau_0 \exp\left(\frac{D_\rho \rho}{\rho_0 - \rho}\right) \quad (28)$$

where $D_\rho$ (isothermal, $D_\rho{}^T$, and isobaric, $D_\rho{}^P$) is a dimensionless parameter and $\rho_0$ is the density at the ideal glass temperature ($T_0$). The parameters used for PEMA with $M_w = 2.0 \times 10^3$ g/mol are as follows: $D_\rho{}^T = 3.94$ and $D_\rho{}^P = 3.25$ for the α-process, $D_\rho{}^T = 1.33$ and $D_\rho{}^P = 1.18$ for the ($\beta\alpha$)-process, and $D_\rho{}^T = 4.6$ and $D_\rho{}^P = 13.2$ for the ion mobility process. $\mathcal{R}$ is then obtained directly at the crossings of the "isotherms" and "isobars", and its $P$- and $T$-dependence is depicted in Figure S3 (bottom). For different ($T-P$)

**Table 3. Ratio of activation energies $\mathscr{R}$ for the four processes observed in PEMA ($M_w = 2.0 \times 10^3$ g/mol) at $P = 0.1$ MPa and $T = 362.15$ K.**

| process | $\mathscr{R}$ ($P$ = 0.1 MPa, $T$ = 362.15 K) |
|---|---|
| $\beta$- | 0.90 |
| α- | 0.60 |
| ($\alpha\beta$)- | 0.68 |
| ion mobility | ~0.65 |

conditions $\mathscr{R}$ is in the range ~0.50−0.70 for the α-process, 0.67−0.77 for the ($\beta\alpha$)-process, 0.67−0.77 for the ion mobility process, and about ~0.9 for the local $\beta$-process (not shown here). The latter is very close to the corresponding values for the $\beta$-process of poly(vinyl chloride)[50] and poly (ethylene terephthalate).[51] Table 3 summarizes the $\mathscr{R}$ values for the four processes obtained in the present study at a common pressure ($P$ = 0.1 MPa) and temperature ($T$ = 362.15 K) lying in the vicinity of their crossing under atmospheric conditions (this procedure involves some extrapolations).

As a consistency check, $\mathscr{R}$ was also calculated by means of eq 7, where $(\partial P/\partial T)_V$ was obtained from $PVT$ measurements and $(\partial T/\partial P)_\tau$ directly from Figure 7 (initial slope). For the α-process using $(\partial P/\partial T)_{V|\tau=100s}$ = 1.9553 MPa/K, and $(\partial T/\partial P)_{\tau=100s} = (\partial T_g/\partial P)_{P\to 0}$ = 0.234 K/MPa, this results in $\mathscr{R}$ = 0.55 ($\tau \sim 100$ s, $P$ = 0.1 MPa); for the ($\beta\alpha$)-process, $(\partial P/\partial T)_{V|\tau=100s}$ = 0.9081 MPa/K, and $(\partial T/\partial P)_{\tau=100s} = (\partial T_g/\partial P)_{P\to 0}$ = 0.254 K/MPa, and $\mathscr{R}$ = 0.77 ($\tau \sim 100$ s, $P$ = 0.1 MPa); and finally for the ionic process, $(\partial P/\partial T)_{V|\tau=100s}$ = 1.6129 MPa/K, $(\partial T/\partial P)_{\tau=100s} = (\partial T_g/\partial P)_{P\to 0}$ = 0.242 K/MPa, and $\mathscr{R}$ = 0.61 ($\tau \sim 100$ s, $P$ = 0.1 MPa).

In addition, Casalini et al.[52] pointed out that the same ratio can be obtained from the ratio of the isobaric, $\alpha_P = (\partial[\ln V]/\partial T)_P$, to the isochronic, $\alpha_\tau = (\partial[\ln V]/\partial T)_\tau$, thermal expansion coefficients as

$$\mathscr{R} = \Delta E^{\#}/\Delta H^{\#} = [1 - \alpha_P/\alpha_\tau]^{-1} \tag{29}$$

Note that eq 29 follows from eq 9 together with eq 24, ignoring the $RT/2$ terms. In these equations, $\alpha_P$ is determined directly from the $PVT$ measurements at $T > T_g$, whereas the isochronal thermal expansion coefficient can be obtained as $\alpha_\tau = \mathrm{d}(\ln V(T_g))/\mathrm{d}T_g(P)$. For the remaining processes, $\alpha_\tau$, was calculated from the $T(P)$ representation (Figure 7) and the relevant Tait parameters. The $\mathscr{R}$ values, thus obtained, amount to 0.55 for the α-process, 0.63 for the ionic process and 0.72 for the ($\alpha\beta$)-process in agreement with the previous estimations.

The results for the α-process make it clear that both temperature and volume are responsible for the slowing down of the segmental dynamics in PEMA with applied pressure. However, between the two variables, it is temperature that exerts the stronger influence. This observation about the dominant effect of thermal energy and the associated energy barriers, correlates nicely with the small volume (~0.17 nm$^3$) of the repeat unit of PEMA as anticipated from the earlier study.[23]

The "ionic" and ($\alpha\beta$)-processes have similar $\mathscr{R}$ values, which are consistently above 0.5, so temperature has the stronger influence on their dynamics. In addition, the similarity of the ratio between the α- and the "mixed" ($\alpha\beta$)-process suggests that the latter has all the characteristics of a structural relaxation to higher temperatures/frequencies. On the other hand, the relative high $\mathscr{R}$ value for the $\beta$-process indicates that the dynamics of this process are governed mainly by thermal effects through the process of groups surmounting intramolecular energy barriers which are strongly perturbed by local packing effects. This is in good agreement with its low apparent activation volume and both ($\Delta V^{\neq}$ and $\mathscr{R}$) support the NMR assignment of a local process.[16,55] Lastly, ions in their motion experience the same local friction as the chain-segments do in the (much faster) ($\alpha\beta$) process. Although the origin of the α-process in PEMA has been discussed earlier,[3b] the origins of the ($\alpha\beta$)- and the "slower" processes in terms of $\Delta V^{\neq}$ and $\mathscr{R}$ were not discussed before in this detail.

## V. Conclusions

We derive the canonical set of equations that describe the effects of the thermodynamic variables $P,V,T$ on average relaxation times. Subsequently, we employ these equations in the investigation of the origin of the different dynamic processes in PEMA. The PEMA dynamics comprise four dielectrically active processes; the segmental (α-) process associated with the liquid-to-glass transition, the local $\beta$-process at lower temperatures, the mixed ($\alpha\beta$)-process at higher temperatures, and a slower process associated with the ion mobility. Pressure aids in clarifying the origin of the dynamic processes by extracting the pressure sensitivity and the relative contribution of thermal energy and volume for each one of the processes.

The α- process bears both intra- and intermolecular contributions and is controlled both by temperature and volume. However, based on the value of the dynamic ratio $\Delta E^{\#}/\Delta H^{\#}$ between the two, it is temperature that exerts the stronger influence. The $\beta$-process, on the other hand, is mainly of intramolecular origin in agreement with earlier NMR results. There is a critical pressure, $P_c(T)$, above which the application of pressure, under "isothermal" conditions, separates the ($\alpha\beta$)- process into the α- and $\beta$-processes. It was found that this critical pressure has a temperature dependence with a coefficient $(\mathrm{d}T/\mathrm{d}P)_c$ ~0.25 K/MPa. Furthermore, the apparent activation volume revealed that the mixed ($\alpha\beta$)-process (at high temperatures/frequencies) is the structural relaxation, implying that it presents characteristics of a segmental process and not of the local $\beta$-process whose apparent activation volume is much smaller (~10−20 cm$^3$/mol). The same conclusion is reached from the values of the ratio of activation energies, $\Delta E^{\#}/\Delta H^{\#}$, with approximate values of 0.60, 0.90, and 0.68, respectively, for the α-, $\beta$- and ($\alpha\beta$)-processes. This value for the ($\alpha\beta$)− process suggest that, while it is controlled both by temperature and volume, the former has the greater influence. Ion mobility, despite being 5 orders of magnitude slower than the ($\alpha\beta$) process, is affected by temperature and volume in the same way as the ($\alpha\beta$) process suggesting that ions in their motion experience a similar local friction.

**Acknowledgment.** K.M. and G.F. acknowledge support by the GSRT programs PENED 529 and 856. We are thankful to Dr. R. Graf (MPI-P) and to Prof. H. W. Spiess (MPI-P) for making available to us the two PEMA samples and for many illuminating discussions.

## Appendix

Cook, Watts and Williams[53] showed for an ensemble of flexible dipolar chain molecules that

$$\left(\frac{\varepsilon^*(\omega) - \varepsilon_\infty}{\varepsilon_0 - \varepsilon_\infty}\right) p(i\omega) = 1 - i\omega \mathscr{J}[C_\mu(t)] \tag{A1}$$

$$C_\mu(t) = \frac{\sum_{ij} \langle \vec{\mu_i}(0)\vec{\mu_j}(t)\rangle}{\sum_{ij} \langle \vec{\mu_i}(0)\vec{\mu_j}(0)\rangle} \tag{A2}$$

where $C_\mu(t)$ is the time correlation function for the angular motions of chain dipoles, $\vec{\mu_i}$, in the ensemble and $p(i\omega)$ is an internal field factor. $C_\mu(t)$ is a weighted sum of auto- and cross-correlation functions, but for flexible chains these have approximately the same time-dependence so $C_\mu(t) \approx \langle \vec{\mu}_i(0)\vec{\mu}_i(t)\rangle/\langle \vec{\mu}_i{}^2\rangle$, the time-autocorrelation function for the motions of a reference chain-dipole. In 1970 Williams[54] introduced the concept of *partial* and *total* relaxations of dipolar groups to rationalize the dielectric $\alpha$,$\beta$ and $\alpha\beta$ processes in amorphous polymers, including the polyalkyl methacrylates. It was assumed the dipole relaxed partially by motions in a temporary local environment with relaxation strength $q_{\beta r} = 1 - (\langle \vec{\mu}_i\rangle_r{}^2)/\mu_i{}^2$ and relaxation function $\varphi_{\beta r}(t)$, where $\langle \vec{\mu}_i\rangle_r$ is the residual dipole moment after local relaxation has occurred. The remaining relaxation strength, $1 - q_{\beta r}$, is relaxed by the $\alpha$-process, with relaxation function $\varphi_\alpha(t)$. Summing up over all initial environments, the following equation was obtained

$$C_\mu(t) = A_\alpha \varphi_\alpha(t) + B_\beta \varphi_\alpha(t)\xi_\beta(t) \qquad \text{(A3)}$$

$A_\alpha = \sum_r p_r^0 q_{\alpha r}$, $B_\beta \xi_\beta(t) = \sum_r p_r^0 q_{\beta r}\varphi_{\beta r}(t)$where $\xi_\beta(t)$ is a weighted sum of relaxation functions for the partial-reorientations of chain dipoles, which relax a portion $B_\beta$ of the total relaxation strength. The $\alpha$-process, due to large-scale micro-Brownian motions of chains, has a relaxation function $\varphi_\alpha(t)$ and relaxes the remaining strength $A_\alpha$, where $A_\alpha + B_\beta = 1$. Equation A3 is sometimes called "the Williams ansatz" It couples together the $\alpha$ and $\beta$ processes when they are due to *motions of the same reference group, but on different time scales*. It predicts *inter alia* that $\alpha$ and $\beta$ processes merge at high temperatures to form the $\alpha\beta$-process, which incorporates the relaxation-strength of the $\alpha$ and $\beta$-processes, and a "conservation rule", $\Delta\varepsilon = \varepsilon_\alpha + \Delta\varepsilon_\beta$, so if $\Delta\varepsilon_\beta$ decreases with increasing pressure, $\Delta\varepsilon_\alpha$ will increase in a complementary manner in order to conserve the total relaxation strength $\Delta\varepsilon$. The functional-forms of the individual relaxations are not specified and are determined by the chemical structure and precise mechanisms for the dynamics of chains for each polymer. Partial reorientations of different chemical groupings in main-chains and side groups (e.g., ester, benzoate) and small pendant groups (e.g., methoxy) will all have different mechanisms, leading to a variety of $\beta$-relaxation processes, as is observed experimentally. Starting with a molecular model for relaxation or using a computer simulation of the dynamics of an ensemble of polymer molecules, the dipole moment time correlation function, $C_\mu(t)$, may be determined using eq A3 for comparison with experimental dielectric data for the $\alpha$,$\beta$ and $\alpha\beta$ processes in amorphous polymers. "Molecular dynamics" computer simulations of the dynamics of models of flexible polymer chains that lead to determinations of $C_\mu$ $(t)$ have been made by several authors, notably by Roe, Binder, Boyd, Smith, Paul, Theodorou, and their co-workers (see refs 56−60 and refs therein).

**Supporting Information Available:** Text giving the derivation of the expressions for the ratio $\mathscr{R}$, as well as further dielectric data including figures showing the effect of pressure on the relaxation curves, the dielectric strength and the activation ratio for each process. This material is available free of charge via the Internet at http://pubs.acs.org.

## References and Notes


(1) McCrum, N. G.; Read, B. E.; Williams, G. *Anelastic and Dielectric Effects in Polymeric Solids*; Wiley: New York, **1991**.
(2) Ishida, Y.; Yamafuji, K. *Kolloid Z*. **1961**, *177*, 97.
(3) (a) Williams, G. *Trans. Faraday Soc*. **1964**, *60*, 1548.(b) Williams, G. *Trans. Faraday Soc*. **1964**, *60*, 1556.
(4) Williams, G. *Trans. Faraday Soc*. **1966**, *62*, 2091.
(5) Williams, G.; Watts, D. C. In *Dielectric Properties of Polymers*; Karasz, F. E., Ed.; Plenum: New York, **1972**; p 17.
(6) Williams, G. *Adv. Polym. Sci*. **1979**, *33*, 60.
(7) Williams, G.; Watts, D. C. In *NMR Basic Principles and Progress*; Diehl, P., Flick, E., Kosfeld, E., Eds.; Springer: Berlin, **1971**; Vol. *4*, p. 271.
(8) Sasabe, H.; Saito, S. *J. Polym. Sci. A-2* **1968**, *6*, 1401.
(9) Ishida, Y. *J. Polym. Sci. A-2* **1969**, *7*, 1835.
(10) Kuebler, S. C.; Schaefer, D. J.; Boeffel, C.; Pawelzik, U.; Spiess, H. W. *Macromolecules* **1997**, *30*, 6597.
(11) Floudas, G.; Stepanek, P. *Macromolecules* **1998**, *31*, 6951.
(12) Schroter, K.; Unger, R.; Reissig, S.; Garwe, F.; Kahle, S.; Beiner, M.; Donth, E. *Macromolecules* **1998**, *31*, 8966.
(13) Beiner, M. *Macromol. Rapid Commun*. **2001**, *22*, 869.
(14) Beiner, M.; Huth, H. *Nat. Mater*. **2003**, *2*, 595.
(15) Gomez, D.; Alegria, A.; Arbe, A.; Colmenero, J. *Macromolecules* **2001**, *34*, 503.
(16) Wind, M.; Graf, R.; Heuer, A.; Spiess, H. W. *Phys. Rev. Lett*. **2003**, *91*, 155702–1.
(17) Wind, M.; Graf, R.; Renker, S.; Spiess, H. W. *Macromol. Chem. Phys*. **2005**, *206*, 142.
(18) Wind, M.; Graf, R.; Renker, S.; Spiess, H. W.; Steffen, W *J. Chem. Phys*. **2005**, *122*, 014906.
(19) Ngai, K. L.; Gopalkrishnan, T. R.; Beiner, M. *Polymer* **2006**, *47*, 7222.
(20) Gaborieau, M.; Graf, R.; Spiess, H. W. *Macromol. Chem. Phys*. **2008**, *209*, 2078.
(21) Arbe, A.; Genix, A.-C.; Colmenero, J.; Richter, D.; Fouquet, P. *Soft Matter* **2008**, *4*, 1792.
(22) *Broadband Dielectric Spectroscopy*, Kremer, F., Schonhals, A., Eds; Springer: Berlin; **2002**.
(23) Floudas, G. *Prog. Polym. Sci*. **2004**, *29*, 1143.
(24) Floudas, G. In ref 22, Chapter 8.
(25) Roland, C. M.; Hensel-Bielowka, S.; Paluch, M.; Casalini, R. *Rep. Prog. Phys*. **2005**, *68*, 1405.
(26) Angell, C. A. *Science* **1995**, *267*, 1924.
(27) Stillinger, F. H. *Science* **1995**, *267*, 1935.
(28) Ferry J. D. *Viscoelastic Properties of Polymers*, 3rd ed.; Wiley: New York, **1980**.
(29) Naoki, M.; Endou, H.; Matsumoto, K. *J. Phys. Chem*. **1987**, *91*, 4169.
(30) Floudas, G.; Mpoukouvalas, K.; Papadopoulos, P. *J. Chem. Phys*. **2006**, *124*, 074905.
(31) Havriliak, S.; Negami, S. *J. Polym. Sci., Part C* **1966**, *14*, 99.
(32) For an account of the different presentations of dielectric data, see: Williams, G.; Thomas, D. K. *Novocontrol Application Notes* No. 3, **1998**.
(33) Zoller, P.; Walsh, D. *Standard pressure-volume-temperature data for polymers*; Technomic publishing Co. Inc.: Lancaster, PA, **1995**, p. 43.
(34) Casalini, R.; Roland, C. M. *Phys. Rev. E* **2004**, *69*, 062501.
(35) Roland, C. M.; Paluch, M.; Pakula, T.; Casalini, R. *Philos. Mag*. **2004**, *84*, 1573.
(36) Barreira, F.; Hills, G. J. *Trans. Faraday Soc*. **1968**, *64*, 1359.
(37) Albuquerque, L. M. P. C.; Reis, J. C. R. *J. Chem. Soc. Faraday Trans*. **1989**, *85*, 207.
(38) Albuquerque, L. M. P. C. *J. Chem. Soc. Faraday Trans*. **1991**, *87*, 1553.
(39) Papadopoulos, P.; Peristeraki, D.; Floudas, G.; Koutalas, G.; Hadjichristidis, N. *Macromolecules* **2004**, *37*, 8116.
(40) Mpoukouvalas, K.; Gomopoulos, N.; Floudas, G.; Herrmann, C.; Hanewald, A.; Best, A. *Polymer* **2006**, *47*, 7170.
(41) Hoffman, J. D.; Williams, G.; Passaglia, E. *J. Polym. Sci., Part C* **1966**, 173.
(42) Dudowicz, J.; Freed, K.; Douglas, J. F. *J. Chem. Phys*. **2005**, *123*, 111102.
(43) Ngai, K. L.; Roland, C. M. *Macromolecules* **1993**, *26*, 6824.
(44) Heijboer, J. Ph.D. Thesis, University of Delft, **1972**.
(45) Paluch, M.; Patkowski, A; Fischer, E. W. *Phys. Rev. Lett*. **2000**, *85*, 2140.
(46) Simon, F. E.; Glatzel, G. Z. *Anorg. Allg. Chem*. **1929**, *178*, 309.
(47) Andersson, S. P.; Andersson, O. *Macromolecules* **1998**, *31*, 2999.
(48) Mpoukouvalas, K.; Floudas, G. *Phys. Rev E* **2003**, *68*, 031801.
(49) Floudas, G.; Gravalides, C.; Reisinger, T.; Wegner, G. *J. Chem. Phys*. **1999**, *111*, 9847.
(50) Williams, G.; Watts, D. C. *Trans. Faraday Soc*. **1971**, *583*, 1971.
(51) Williams, G. *Trans. Faraday Soc*. **1966**, *62*, 1321.
(52) Casalini, R.; Roland, C. M. *J. Chem. Phys*. **2003**, *119*, 4052.
(53) Cook, M.; Watts, D. C.; Williams, G. *Trans. Faraday Soc*. **1970**, *66*, 2503.

(54) Williams, G. *Chem. Rev.* **1972**, *72*, 55.
(55) Bonagamba, T. J.; Becker-Guedes, F.; DeAzevedo, E. R.; Schmidt-Rohr, K *J. Polym. Sci. Polym. Phys. Ed.* **2001**, *39*, 2444.
(56) (a) Roe, R. J. *Adv. Polym. Sci.* **1994**, *116*, 111.(b) *J. Non Cryst. Solids* **1995**, *172*−*177*, 77.
(57) (a) Binder, K., Ed. *Monte Carlo and Molecular Dynamics Simulations in Polymer Science*; Oxford University Press: Oxford, U.K., **1995**. (b) Binder, K.; Paul, W. *J. Polym. Sci., Polym. Phys.* **1997**, *35*, 1.
(58) Paul, W.; Smith, G. D. *Rep. Prog. Phys.* **2004**, *67*, 1117.
(59) Smith, G. D.; Bedrov, D. *J. Polym. Sci., Polym. Phys.* **2007**, *45*, 627.
(60) Boyd, R. H.; Smith, G. D. *Polymer Dynamics and Relaxation*; Cambridge University Press: Cambridge, U.K., **2007**.